Analytical Solution to Global Dynamic Balance Control of the Acrobot

Xiaojiao Chen, *Student Member, IEEE,* Tommy Hu, Chaoyang Song, *Member, IEEE,* and Zheng Wang*, *Senior Member, IEEE*

Abstract— To provide a high level dynamic stability objective for humanoid robots that takes into consideration forces due to joint coupling, we derive an analytical solution to the dynamic balance control of the Acrobot, a fixed-base underactuated inverted double pendulum. We will show that the proof for stability involves an analogy to the dynamic stabilization of a rigid pendulum through vertical vibrations of its base, thus providing physical and mathematical insights into controls and dynamic stability of underactuated, articulated systems like the humanoid robot.

I. INTRODUCTION

Humanoid robots generally take behavioral compliance approaches to achieve smooth, natural, and safe operations both for locomotion and for manipulation tasks [1-8]. Unlike soft robots with compliant [9-11] or hybrid bodies [12-16], rigid-bodied humanoid robots must be specifically controlled to achieve satisfactory results. One of the prerequisites for humanoid robots performing any task is that they do not fall over either due to external disturbances or in the process of executing desired motions. These desired motions may include complex gait planning or upper body manipulation tasks, and external disturbances may result from interaction with dynamic environments with unexpected environmental forces or traversal of difficult terrain. As such, the humanoid robot must autonomously plan while considering stability as well as have a mechanism to control for disturbances.

A method used to ensure this stability is to depict representative elements of the humanoid dynamics such as the center of mass (CoM), the center of pressure (CoP), or the Zero Moment Point (ZMP)[1] using a simplified model, then map the desired dynamics of the simplified model back to the full dynamic model of the humanoid by solving an inverse kinematics or by using some other optimization based method[2], [3]. In recent years, optimization methods such as quadratic programming approaches[4] have been able to generalize algorithms based on these CoM and ZMP planning techniques to offer increasingly rapid and robust whole-body control and planning solutions[5]–[7]. However, numerical and computational complexity, local minima solutions, and the 'black/gray box' nature of these methods are just some of the many problems that remain unsolved. As noted by[8], one of the keys to solving these issues is to improve understanding of the underlying physics and dynamics involved in stability and to exploit resulting mathematical structures.

The linear inverted pendulum model (LIPM)[17], [18] and its many variations such as the Reaction Mass Pendulum (RMP)[19] and other extensions that incorporate angular momentum[6], [20] have been able to provide sufficiently complex yet tractable representation of the physics of the stability of humanoid robots. As a result, this approach has had wide applications in humanoid robot balancing, fall detection, push recovery, footstep/gait planning, and walking pattern generation. The Acrobot is a fixed-base inverted double pendulum that is unactuated at the base joint[21]. A typical example of a chaotic system, the inverted double pendulum and its control methodologies have interested many robotics researchers specifically for application to standing postural control in machines and animals[8]. In terms of dynamics, it builds on developments of inverted pendulum models by allowing for explicit consideration of torque interaction between the two linkages of the double pendulum. The importance of forces arising from linkage interactions in humanoid robots can be seen in the biomechanics of arm-swinging motions for dynamic walking[22], [23] and hip/ankle strategies in human balance[24]. The unactuated joint of the Acrobot further captures the underactuated nature of bipedal robots in which the contact between the foot and the ground cannot be directly controlled.

Typically, controllers for the Acrobot have focused on swing-up control[25], which is not suitable for humanoid applications. Still, many analytical techniques have been proposed to tackle balance control of the Acrobot, usually based on generation of inputs that neutralize system drift vector fields, but these are typically valid only in in areas relatively close to the statically unstable inverted equilibrium posit ion. Linear quadratic regulator (LQR) methods[26], [27] or other optimal regulator functions combined with linear feedback [28] have provided asymptotic stabilization, but with regions of attraction that are unsatisfactorily small. Genetic algorithms[29], learning techniques[30], and optimization-based methods[8] have achieved some successes but often cannot provide stability performance guarantees due to issues such as singularities, slow speeds hindering online implementation, and the lack of direct contribution to understanding the underlying dynamics of Acrobot balancing.

In this work, we present an analytical solution to the global dynamic balance control of the Acrobot and provide a proof for global dynamic stability based off an analogy to the dynamic stabilization of the Kapitza pendulum[31], a rigid pendulum vertically vibrating at its base. Our method allows for postural control in any state of the system based on physical properties of the Acrobot, thus suggesting underlying properties that may be directly applicable to dynamical systems of similar articulated structures. In contrast to the

X. Chen, T. Hu and Z. Wang are with the Department of Mechanical Engineering. Faculty of Engineering, The University of Hong Kong, China (chen2014, hutommy, zwangski) @hku.hk

C. Song is with the Department of Mechanical and Energy Engineering, Southern University of Science and Technology, Shenzhen, China songcy@sustc.edu.cn

Z. Wang is also with the University of Hong Kong Shenzhen Institute of Research and Innovation (HKU-SIRI), Shenzhen, China

* Author of correspondence, zwangski@hku.hk

static or quasi-static stability restriction of many humanoid robot control methods, the global dynao1ic stability property of our control law means that the center of mass of the Acrobot system can be kept permanently away from the system base with the system remaining stable only through dynamic motions of the active upper joint, thus extending the realm of trackable trajectories or motions and also suggesting possibility for faster motions that were not possible with statically or quasi-statically stable methods.

II. CONTROL LAW DERIVATION

We begin by examining the equations of motion for a fully actuated double pendulum

$$\begin{bmatrix} M_{aa} & M_{ap} \\ M_{pa} & M_{pp} \end{bmatrix} \begin{bmatrix} \ddot{\theta}_a \\ \ddot{\theta}_p \end{bmatrix} + \begin{bmatrix} b_a \\ b_p \end{bmatrix} = \begin{bmatrix} \tau_a \\ \tau_p \end{bmatrix} \quad (1)$$

Where θ_a corresponds to the active joint angles, θ_p to the passive ones, M is the inertia matrix with indices according to the variables they relate and is symmetric and positive definite, b contains expressions for gravitational forces as well as nonlinear velocity effects including centrifugal and Coriolis forces, and τ_a and τ_b are the torques exerted by the active and passive joints, respectively. We note that, in the case of the equations of motion for the Acrobot, the passive joint does not exert any torque and thus we have the above but with $\tau_p = 0$.

By multiplying out the equations of motion for an Acrobot, i.e. Equation (1) with $\tau_p = 0$, we can write

$$M_{aa}\ddot{\theta}_a + M_{ap}\ddot{\theta}_p + b_a = \tau_a \quad (2)$$
$$M_{pa}\ddot{\theta}_a + M_{pp}\ddot{\theta}_p + b_p = 0 \quad (3)$$

Solving for the active joint acceleration $\ddot{\theta}_a$ in (2) and the passive joint acceleration $\ddot{\theta}_p$ in (3) yields

$$\ddot{\theta}_a = -M_{aa}^{-1}M_{ap}\ddot{\theta}_p - M_{aa}^{-1}b_a + M_{aa}^{-1}\tau_a \quad (4)$$
$$\ddot{\theta}_p = -M_{pp}^{-1}M_{pa}\ddot{\theta}_a - M_{pp}^{-1}b_p \quad (5)$$

The terms $-M_{aa}^{-1}M_{ap}\ddot{\theta}_p$ and $-M_{pp}^{-1}M_{pa}\ddot{\theta}_a$ in (4) and (5) can be viewed as the virtual acceleration[24] of the active joint generated by the acceleration of the passive one, and vice versa, respectively. We assume that the active joint and the passive joint are coupled, which means that the off-diagonal elements of the inertia matrix, M_{ap} and M_{pa}, are non-zero. We will let (4) and (5) represent the resulting acceleration due to input into the system, which include the expressions on the right-hand-side. As such, we will let the passive joint acceleration be zero, i.e. $\ddot{\theta}_p = 0$, in (4), since the passive joint cannot actively exert torque to produce acceleration, and we use the substitution $M_{aa}^{-1}\tau_a = \ddot{\bar{\theta}}_a$, where $\ddot{\bar{\theta}}_a$ is the active joint acceleration produced by the exerted torque. The actual value of the virtual acceleration of the active joint due to the current acceleration of the passive joint will be taken into consideration later when we derive the torque necessary to produce the desired active joint acceleration, $\ddot{\bar{\theta}}_a$. We also make the substitution $\ddot{\theta}_a = \ddot{\bar{\theta}}_a$ in (5) because $\ddot{\bar{\theta}}_a$ is the actual input acceleration of the active joint that will create the virtual acceleration of the passive joint, yield

$$\ddot{\theta}_a = \ddot{\bar{\theta}}_a + B_a \quad (6)$$
$$\ddot{\theta}_p = M_p\ddot{\bar{\theta}}_a + B_p \quad (7)$$
$$B_a \equiv -M_{aa}^{-1}b_a; \ B_p \equiv -M_{pp}^{-1}b_p; \ M_p \equiv -M_{pp}^{-1}M_{pa}.$$

The values of B_a, B_p, and M_p only depend on the joint angles and the joint velocities of the Acrobot, θ_{Acrobot} and
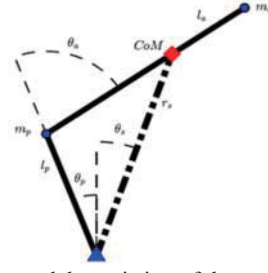

Fig. 1. The Acrobot model consisting of the proximal passive link and a distal active link and configurable inertial properties. The dotted line indicates the schematic for the equivalent CoM SIP.

$\dot{\theta}_{\text{Acrobot}}$, and is completely determined once measurements of these variables are available. Equation (6) and (7) take a desired input acceleration to the active joint and produces the output acceleration in both the active and the passive joints. We note that in its current state, (6) and (7) do not consider the virtual accelerations due to current accelerations but only the virtual accelerations due to explicitly input accelerations and torques. The virtual accelerations will be dealt with when the active joint torque τ_a required to produce the desired active joint acceleration $\ddot{\theta}_a$ is derived.

We can imagine that an inverse of the formulation of (6) and (7) is able to take desired joint accelerations as input and output required active joint accelerations and thus allows us to deal with the underactuated aspect of the Acrobot. If we have command accelerations to both the active and the passive joints that will stabilize the system, we can realize acceleration using only torque input to the active joint.

We control the Acrobat's joint angles θ_a and θ_p by controlling the tangential and radial forces on the endpoint of a single inverted pendulum (SIP) of variable length whose endpoint properties including mass m_s, angular position θ_s, angular velocity $\dot{\theta}_s$, radial position T_s, and radial velocity r_s correspond to the total mass, CoM angular position θ_{CoM}, CoM angular velocity $\dot{\theta}_{CoM}$, CoM radial position r_{CoM}, and CoM radial velocity $\dot{r}_{CoM}$ of the Acrobot, respectively. In contrast to the LIPM, there is no restriction placed on the endpoint of the SIP, and thus the endpoint can freely move in any direction. The torques on the system $\tau_{s\theta}$ and the radial force F_{sr} for the CoM SIP of variable length is described as

$$\tau_{s\theta} = F_{s\theta}r_s = I_s\alpha_{s\theta} = -m_s g s(\theta_s) - m_s r_s \dot{\theta}_s \dot{r}_s + T_s \quad (8)$$
$$F_{sr} = m_s a_{sr} = -m_s g c(\theta_s) - m_s r_s \dot{\theta}_s^2 + R_s \quad (9)$$
$$c(x) \equiv \cos(x), \ s(x) \equiv \sin(x),$$

where g is gravity, I_s is the moment of inertia of the SIP, m_s is the total mass of the Acrobat $m_p + m_a$, θ_s is the angle from the origin of the CoM SIP, $\dot{\theta}_s$ is the angular velocity of the CoM SIP, and F_r is the desired radial direction force input to the system. The variables T_s and R_s represent respectively the torque and radial force input used to control the system.

The location, velocity, and acceleration of the CoM of the Acrobat can be expressed in Cartesian coordinates by the CoM Jacobian J_{CoM} and the CoM Jacobian rate of change $\dot{J}_{CoM}$:

$$x_{CoM} = \begin{bmatrix} x_{CoM} \\ y_{CoM} \end{bmatrix} = \begin{bmatrix} \dfrac{-l_p m_p s(\theta_p) + m_a\left(-l_p s(\theta_p) - l_a s(\theta_p + \theta_a)\right)}{m_p + m_a} \\ \dfrac{l_p m_p c(\theta_p) + m_a\left(l_p c(\theta_p) + l_a c(\theta_p + \theta_a)\right)}{m_p + m_a} \end{bmatrix} \quad (10)$$

$$\dot{\boldsymbol{x}}_{CoM} = \begin{bmatrix} \dot{x}_{CoM} \\ \dot{y}_{CoM} \end{bmatrix} = \boldsymbol{J}_{CoM}\dot{\boldsymbol{\theta}}_{Acrobot} \qquad (11)$$

$$\ddot{\boldsymbol{x}}_{CoM} = \begin{bmatrix} \ddot{x}_{CoM} \\ \ddot{y}_{CoM} \end{bmatrix} = \boldsymbol{J}_{CoM}\ddot{\boldsymbol{\theta}}_{Acrobot} + \dot{\boldsymbol{J}}_{CoM}\dot{\boldsymbol{\theta}}_{Acrobot} \qquad (12)$$

and the structure of the CoM Jacobian is the partial derivative of the location of the CoM of the Acrobat with respect to the joint angles and the CoM Jacobian rate of change is the partial derivative of the CoM Jacobian with respect to the joint angles:

$$\boldsymbol{J}_{CoM} = \frac{\partial \boldsymbol{x}_{CoM}}{\partial \boldsymbol{\theta}_{CoM}} \qquad (13)$$

$$\dot{\boldsymbol{J}}_{CoM} = \frac{\partial \boldsymbol{J}_{CoM}}{\partial \boldsymbol{\theta}_{CoM}} \qquad (14)$$

The angular acceleration of the CoM SIP can then be derived by inserting the expressions for the variables involved in x_{CoM}, $\dot{x}_{CoM}$, and $\ddot{x}_{CoM}$ into the expression for the angular velocity and angular acceleration of the of the CoM SIP, which is simply the second derivative of the equation for the angular position $\theta = -\arctan\left(\frac{x}{y}\right)$, yielding

$$\dot{\theta} = \frac{x\dot{y} - \dot{x}y}{x^2 + y^2} \qquad (15)$$

$$\ddot{\theta} = \frac{2(x\dot{x} + y\dot{y})(-x\dot{y} + \dot{x}y) + (x\ddot{y} - \ddot{x}y)(x^2 + y^2)}{(x^2 + y^2)^2} \qquad (16)$$

The expressions for the terms in x_{CoM} and $\dot{x}_{CoM}$ are completely determined after the state measurements $\theta_{Acrobot}$ and $\dot{\theta}_{CoM}$ of the Acrobat are available, and thus we can express the angular acceleration of the CoM SIP in terms of the Acrobat joint angular accelerations as

$$\ddot{\theta}_{CoM} = A\ddot{\theta}_a + P\ddot{\theta}_p + O \qquad (17)$$

where A and P contain all the terms involving $\ddot{\theta}_a$ and $\ddot{\theta}_p$ respectively after substitution of the variables in (8), (9), and (10) into (14) with their respective multipliers factored out, and O contains all the remaining terms in the result of the substitution. Hence, we can describe the angular acceleration of the CoM SIP using angular accelerations of the Acrobat.

We will let the variable $\ddot{\theta}_{CoM}$ be our desired CoM angular acceleration, $\ddot{\theta}_{CoM,desired}$. The desired CoM angular acceleration is described by the effects in (8) by $\alpha_{s\theta}$. We negate the signs of the gravitational and Coriolis effects (since we are trying to overcome them) in (7) while keeping the positive sign convention a command torque input T_s to yield

$$\ddot{\theta}_{CoM,desired} = I_s^{-1}\left(m_s g s(\theta_s) + m_s r_s \dot{\theta}_s \dot{r}_s + T_s\right) \qquad (18)$$

which can then be substituted into (16).

There are no singularities in (16) for nonzero Acrobat length and mass, as we can imagine that at any position angular acceleration of either the active joint or the passive joint will affect an angular acceleration of the CoM SIP. However, the same cannot be said about a similar derivation for the radial direction acceleration of the endpoint of the CoM SIP in terms of the Acrobat's joint angular accelerations, as an angular acceleration of either joint of the Acrobat when the two linkages are aligned and at the straight-up-and-down position is not able to command any radial-direction acceleration of the CoM SIP. As such, we utilize a derivation like an attachment of a virtual structure used by Pratt et al. for virtual model control[33]. Avoiding the singularity is accomplished by attaching horizontal and vertical forces F_{cx} and F_{cy} that act on the CoM of the Acrobat at any point in time. These are simply additional input forces on the equations of motion for the Acrobat, and considering their effects, (6) and (7) become
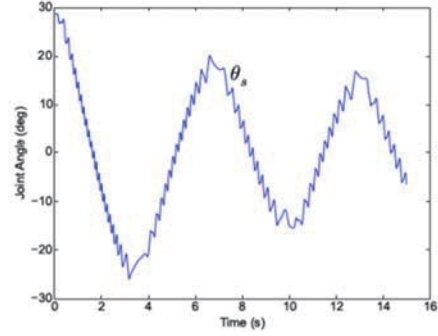

Fig. 2. Angular position of equivalent CoM SIP superposition of two sinusoids with different amplitude/ frequencies.

$$\ddot{\theta}_a = \ddot{\bar{\theta}}_a + C_{afx}F_{cx} + C_{afy}F_{cy} + B_a \qquad (19)$$

$$\ddot{\theta}_p = M_p\ddot{\bar{\theta}}_a + C_{pfx}F_{cx} + C_{pfy}F_{cy} + B_p \qquad (20)$$

Where

$$C_{afx} \equiv -\frac{c(\theta_p + \theta_a)}{l_a(m_p + m_a)} \quad C_{afy} \equiv -\frac{s(\theta_p + \theta_a)}{l_a(m_p + m_a)}$$

$$C_{pfx} \equiv -\frac{l_p m_p c(\theta_p) + l_p m_a c(\theta_p) + l_a m_a c(\theta_p + \theta_a)}{D}$$

$$C_{pfy} \equiv -\frac{l_p m_p s(\theta_p) + l_p m_a s(\theta_p) + l_a m_a s(\theta_p + \theta_a)}{D}$$

$$D \equiv l_p^2 m_p^2 + 2l_p^2 m_p m_a + l_p^2 m_a^2 + 2l_p m_p m_a c(\theta_a)$$
$$+ 2l_p l_a m_a^2 c(\theta_a) + l_a^2 m_p m_a + l_a^2 m_a^2$$

Then, we again negate the expressions for the gravitational force and the centripetal force in the radial direction from (9) while keeping the sign of R_s the same, and project these radial forces onto the x- and y-axes to obtain the desired radial input forces. We can then rearrange to isolate our desired radial direction input force R_s to yield

$$F_{cx} = -R_s s(\theta_s) - G_s(\theta_s) \qquad (21)$$

$$F_{cy} = R_s c(\theta_s) + Gc(\theta_s) \qquad (22)$$

$$G \equiv m_s g c(\theta_s) + m_s r_s \dot{\theta}_s^2.$$

Now, to put everything together, we first substitute the expression for F_{cx} and F_{cy} in (21) and (22) into (17) and get

$$\ddot{\theta}_a = \ddot{\bar{\theta}}_a - (R_s + G)(C_{axs} - C_{ayc}) + B_a \qquad (23)$$

$$\ddot{\theta}_p = M_p\ddot{\bar{\theta}}_a - (R_s + G)(C_{pxs} - C_{pyc}) + B_p \qquad (24)$$

$$C_{axs} \equiv C_{afx}s(\theta_s), C_{ayc} \equiv C_{afy}c(\theta_s)$$

$$C_{pxs} \equiv C_{pfx}s(\theta_s), C_{pyc} \equiv C_{afy}c(\theta_s).$$

Then substitute the expression for $\ddot{\theta}_a$ and $\ddot{\theta}_p$ in (23) and (24) into (16) with the desired CoM angular acceleration described in (18) and isolate $\ddot{\bar{\theta}}_a$ to obtain

$$\ddot{\bar{\theta}}_a = \frac{I_s^{-1}(E + T_s) + (R_s + G)C_{AP} - B_{AP} - O}{A + M_p P} \qquad (25)$$

$$E \equiv m_s g s(\theta_s) + m_s r_s \dot{\theta}_s \dot{r}_s;$$

$$C_{AP} \equiv A(C_{axs} - C_{ayc}) + P(C_{pxs} - C_{pyc});$$

$$B_{AP} \equiv AB_a + PB_p$$

The expression in the denominator of (25) is always nonzero, and thus the expression is safe from singularities. Equation (25) gives us a command of Acrobot active joint acceleration given a desired input torque T_s and input radial force R_s to the equivalent CoM SIP. Then the torque input to

the Acrobot τ_a is calculated from the desired angular acceleration $\ddot{\theta}_a$ by substituting the virtual acceleration of the passive joint in (5) into the motion equation for the active joint in (2)

$$\tau_a = M_{aa}\ddot{\theta}_a + M_{ap}\left(-M_{pp}^{-1}M_{pa}\ddot{\theta}_a - M_{pp}^{-1}b_p\right) + b_a \quad (26)$$

The control law for T_s and R_s to stabilize the CoM SIP derived from the Acrobot is

$$T_s = -K_{p\theta}(\theta_s - \theta_{sdes}) - K_{d\theta}\dot{\theta}_s \quad (27)$$
$$R_s = -K_{pr}(r_s - r_{des}) - K_{dr}\dot{r}_s \quad (28)$$

where $K_{p\theta}$ and K_{pr} are the proportional gains for the angular and radial positions and $K_{d\theta}$ and K_{dr} are the derivative gains for the angular and radial velocities.

Using the above control law with gains $K_{p\theta} = 200$, $K_{v\theta} = 100$, $K_{pr} = 0$, $K_{vr} = 100$ on a simulated Acrobot with initial joint angles $\theta_p = 28°$, $\theta_a = 0$ and zero initial joint velocities, the active joint of the Acrobot spins like the blades of a fan, driving the passive joint to oscillate rotationally, which in turn drives an overall movement of the entire Acrobot. The overall effect can be summarized by plotting the angular position of the motion of the equivalent CoM SIP, as shown in Fig. 2. Note that the figure resembles the combination of two waveforms, one with smaller amplitude and larger frequency representing the rapid effects of the spinning active joint, and the other a large amplitude, lower frequency waveform representing the overall motion of the system that seems to be diminishing as time increases. This insight will aid the next section in proving the global dynamic stability of the Acrobot controlled by (27) and (28).

III. PROOF OF STABILITY BY THE GENERALIZED KAPITZA METHOD

The Kapitza pendulum, named after Russian Nobel laureate physicist Pyotr Kapitza, refers to an inverted pendulum that is stabilized in the inverted position by vertical vibrations at its pivot point. Intuitively, the stability occurs due to a shorter moment arm during the downward motion of the vibration relative to the upward motion of the vibration, thus causing an overall moment moving the pendulum to the inverted position. Mathematically, Kapitza pendulum stability can be proved in two ways. The first utilizes Floquet theory on the Mathieu equation, thus demonstrating the disturbance rejection abilities of the Kapitza pendulum and allowing for the stability regions of the pendulum to be illustrated on a graph of frequency of vibration versus amplitude of vibration[34]. The second method is by Kapitza and involves deriving the effective potential towards which the system converges by decomposing the effects of the vertical vibrations into 'slow' and 'fast' components and then time-averaging over the rapid oscillations[31]. We use a generalization of the second method that generalizes the inverted pendulum into an arbitrary particle acted on by an arbitrary periodic force[35].

We begin by recalling that a periodic force $F(x,t)$ can be defined in terms of a Fourier series as

$$F(x,t) = \sum_{k=1}^{\infty}[a_k(x)\cos(k\omega t) + b_k(x)\sin(k\omega t)] \quad (29)$$

the Fourier coefficients $a_k(x)$ and $b_k(x)$ are given by

$$a_k(x) = \frac{2}{T}\int_0^T f(x,t)\cos(k\omega t)\,dt \quad (30)$$

$$b_k(x) = \frac{2}{T}\int_0^T f(x,t)\sin(k\omega t)\,dt \quad (31)$$

We then rewrite the motion of the endpoint of our Acrobat Equivalent CoM SIP in terms of the motion for an arbitrary particle of mass m that is governed by

$$m\ddot{x} = -\frac{dU(x)}{dx} + F(x,t) \quad (32)$$

where $dU(x)/dx$ is the force due to a time-independent potential field $U(x)$, and $F(x,t)$ is periodic. We observe in $x(t)$ a fast $\xi(t)$ and a slow component $X(t)$, yielding

$$x(t) = X(t) + \xi(t) \quad (33)$$

We assume that the mean value of the fast component $\xi(t)$, over its period T is zero, and that the slow component $X(t)$ is more or less constant over that time. We take the first order Taylor's expansion of the motion over a small time-step equivalent to the fast component to yield

$$\frac{dU}{dx} = \frac{dU}{dX} + \xi\frac{d^2U}{dX^2} \quad (34)$$

$$F(x,t) = F(X,t) + \xi\frac{dF}{dX} \#(35)$$

Substituting this into (32) yields

$$m\ddot{X} + m\ddot{\xi} = -\frac{dU}{dX} - \xi\frac{d^2U}{dX^2} + F(X,t) + \xi\frac{dF}{dX} \quad (36)$$

We let the fast component of the motion be a result of the periodic force to obtain

$$m\ddot{\xi} = F(X,t) \quad (37)$$

and then integrate while regarding X as a constant to yield

$$\xi = -\frac{1}{m\omega^2}\sum_{k=1}^{\infty}\frac{1}{k^2}[a_k\cos(k\omega t) + b_k\sin(k\omega t)] \quad (38)$$

We subtract the value of the fast component defined in (37) from the Taylor expansion expression in (36) to yield the slow component of the motion

$$m\ddot{X} = -\frac{dU}{dX} - \xi\frac{d^2U}{dX^2} + \xi\frac{dF}{dX} \quad (39)$$

Time-averaging the Taylor expansion in (36) over the time period T and using the facts that $\bar{\xi} = 0$, $\overline{F(X,t)} = 0$ and the slow components assumed constant over the interval T yields

$$m\ddot{X} = -\frac{dU}{dX} + \overline{\xi\frac{dF}{dX}} \quad (40)$$

where the bar-notation designates an average value over the time period T. We can differentiate (29) to obtain

$$\frac{dF}{dX} = \sum_{k=1}^{\infty}\left[\frac{da_k}{dX}\cos(k\omega t) + \frac{db_k}{dX}\sin(k\omega t)\right] \quad (41)$$

and since the value of ξ is known from (38), we can obtain

$$\overline{\xi\frac{dF}{dX}} = -\frac{1}{m\omega^2}\sum_{k,j=1}^{\infty}\frac{1}{k^2}[\,a_k\frac{da_j}{dX}\overline{\cos(k\omega t)\cos(j\omega t)}$$

$$+b_k\frac{da_j}{dX}\overline{\sin(k\omega t)\cos(j\omega t)} + a_k\frac{db_j}{dX}\overline{\cos(k\omega t)\sin(j\omega t)}$$

$$+b_k\frac{db_j}{dX}\overline{\sin(k\omega t)\sin(j\omega t)} \quad (42)$$

Then, for $k = j$ we have

$$\overline{\sin(k\omega t)\cos(j\omega t)} = \overline{\cos(k\omega t)\sin(j\omega t)} = 0 \quad (43)$$

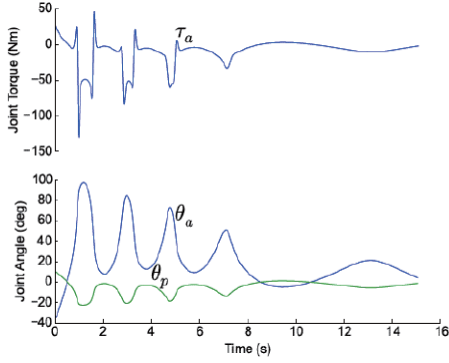$$\overline{\cos(k\omega t)\cos(j\omega t)} = \overline{\sin(k\omega t)\sin(j\omega t)} = \frac{1}{2} \quad (44)$$

Fig. 3. Example 1. Initially unstable position of the Acrobot system dynamically stabilized using oscillatory inputs.

Fig. 4. Example 2. The system also attempts to dynamically stabilize with regards to the three seconds of disturbance.

and for $k \neq j$ the terms are zero. This gives us

$$\overline{\xi \frac{dF}{dX}} = -\frac{1}{4m\omega^2} \sum_{k=1}^{\infty} \frac{1}{k^2} \left(\frac{da_k^2}{dX} + \frac{db_k^2}{dX} \right) \quad (45)$$

which can be substituted into (40) to yield

$$m\ddot{X} = -\frac{dU}{dX} - \frac{1}{4m\omega^2} \sum_{k=1}^{\infty} \frac{1}{k^2} \frac{da_k^2 + db_k^2}{dX} \quad (46)$$

which only contains two terms that are both differentials, and thus can be written as

$$m\ddot{X} = -\frac{d}{dX} \left(U + \frac{1}{4m\omega^2} \sum_{k=1}^{\infty} \frac{a_k^2 + b_k^2}{k^2} \right) = -\frac{dU_{eff}}{dX} \quad (47)$$

where U_{eff} is the effective potential. Like any other potential function, the system converges to the minimum of the effective potential function, and thus the system is globally stable if that minimum is stable. Thus the stability of the system is determined by the Fourier coefficients of the forcing function.

To apply this to our Acrobot control method, we determine the torque about the base link instead of the endpoint of the passive joint for the input defined in (26) and divide by the instantaneous length of the CoM, r_s, to yield an equivalent tangential and radial force at the CoM. Then, we can apply the generalized Kapitza method proof method in both directions to yield tangential and radial effective potential functions. Since the torque input function itself is a differential equation without an analytical solution, we cannot readily solve for the values of the gains given a desired point of convergence. However, we can still calculate an effective potential using the discrete Fourier series of the results of numerical solution to the differential equation and obtain data for a set of initial Acrobot joint conditions, gains, and resulting convergence. The Acrobot controller design problem is then reduced to determining the range of initial Acrobot joint conditions we want to design for and selecting the set of gains that will provide the desired convergence behavior both in the tangential and the radial direction for the desired range. Furthermore, we also observed during the tuning that the effects of the individual gains also correspond to the variables they modify. For example, tuning K_{pr} corresponds to forcing the Acrobot to 'extend' so as to elongate the distance between its CoM and the base, and thus if K_{pr} is set to zero the final statically unstable equilibrium position of the Acrobot may correspond to one in which the Acrobot is 'hunched over'.
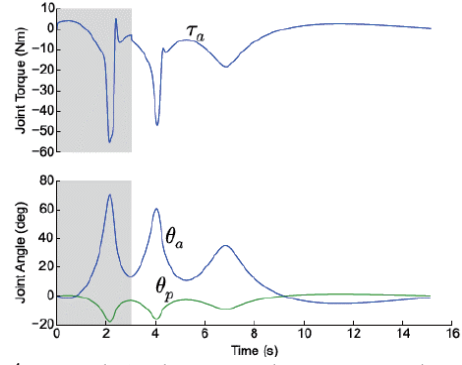
IV. SIMULATION RESULTS

We simulated the Acrobot with inertial parameters $l_p = 0.75$, $l_a = 0.5$, $m_p = 7$, $m_a = 8$ with various initial angular positions as well as with an initially stable position subject to disturbances. Using gains of $K_{p\theta} = K_{v\theta} = 900$, $K_{pr} = 350$, $K_{vr} = -900$ and the desired angular position and velocity set to the stable inverted position, the control law was able to bring the system to an inverted equilibrium position from any initial angular position or velocity. However, with initial positions that are extremely far away from the initial position such as with $\theta_p > 60$, $\theta_a = 0$ or with both linkages parallel to the ground, we observe motion where the active joint spins like a fan to cause the entire system to rotate towards the equilibrium position and then transitions into a more reasonable trajectory of oscillations to the inverted equilibrium when it is near the inverted position before settling stably. Fortunately, the conditions where this 'helicopter' action takes place is way outside any humanoid robot and thus can be easily avoided.

Fig.3 shows results for an initial condition of $\theta_p = 10°$, $\theta_a = -35°$, $\dot{\theta}_p = \dot{\theta}_a = 0$, a reasonable state for humanoid representation far away from the inverted equilibrium position. The control law initially exerts a large torque through a twist at the waist to force the system away from the instability-causing effects of gravity into a dynamically stable state, as demonstrated by the initial crossover between the θ_a and θ_p from negative to positive and vice versa, respectively. Then, the torque input τ_a oscillates with diminishing amplitude as it brings the system from non-stationary dynamic equilibrium to the statically unstable equilibrium at the inverted position.

Fig. 4 shows results for the system initially in the static inverted position of $\theta_a = \theta_p = 0°$ subject to a 5N force at the endpoint of the distal linkage for 3 seconds, as indicated by the shaded area. We can see that the torque input is also oscillatory in nature with decreasing amplitude with respect to the effects of the disturbance. If the disturbance were to persist, the system would transition from the dynamic equilibrium with the disturbance to a statically unstable equilibrium position that balances out the disturbance. As the disturbance was removed at time t = 3, the torque input went from oscillatory inputs with respect to the disturbance to oscillatory inputs that regulate the effects of gravity as in the previous example, eventually settling into the original inverted position.

These results concur with the proof from the previous section for stability based on viewing the input effects as a sinusoid. This provides strong rationale for further

investigation of the model and control method for humanoid periodic locomotion applications such as dynamic running pattern generation. Furthermore, the proof for stability and the simulation results also provide an analytical basis for the oscillatory input found by stochastic programming with respect to the Larangian in[8] for control of a spatial inverted double pendulum, and possible further theoretical extensions and generalizations through steering by sinusoids for nonholonomic systems in[36].

V. CONCLUSION

We considered the problem of balance control of the Acrobot as a model for humanoid balancing for its ability to capture dynamical features such as nonlinear velocity effects lost in simpler single inverted pendulum models. The proceeding derivation of the control law and the proof for stability not only allows for global stability, but also provides a significant amount of physical insight into the nature of the dynamic balancing of underactuated articulated bodies like the humanoid robot, an aspect that is missing in many purely optimization-based or learning methods. By incorporating the dynamics of inertial coupling between the joints, we could include an expression for the virtual acceleration of the passive joint into the dynamics of the active joint so it can take responsibility for the under actuation as it moves. Then, by noticing the differences in speeds induced by the actuation, we proved the stability of the Acrobot system by decomposing the input force into sinusoids of two time-scales of movement and integrating over the period to examine the overall motion.

Since the requirement for arriving at an effective potential function indicative of successful global stabilization is only a periodic input, we wish to explore modifications to the trajectories as the system stabilizes through alternative control law derivations to minimize other performance metrics such as overall energy input through means such as passivity-based controls. Naturally, we intend to explore how this model can contribute to current state-of-the-art control methodologies for humanoid robot whole-body motion planning and control, with emphasis placed on how the ideas on dynamic stability gained from this work allows for a wider range of motions and improved stability as well as improvements on computational efficiency possibly by exploiting harmonic structures in solutions. Finally, we also intend for the control ideas introduced to be extended into a three-dimensional version of the Acrobot such as the spatial inverted double pendulum and toward more complex versions with more joints, and eventually to a full dynamics model of a humanoid robot.

REFERENCES

[1] M. VUKOBRATOVIĆ and B. BOROVAC, "Zero-Moment Point — Thirty Five Years of Its Life," *Int. J. Humanoid Robot.*, vol. 1, no. 1, pp. 157–173, 2004.

[2] S. Kajita *et al.*, "Biped walking pattern generation by using preview control of zero-moment point," *Robot. Autom. (ICRA), IEEE Int. Conf.*, vol. 2, pp. 1620–1626, 2003.

[3] K. Nishiwaki, S. Kagami, Y. Kuniyoshi, M. Inaba, and H. Inoue, "Online generation of humanoid walking motion based on a fast generation method of motion pattern that follows desired ZMP," *IEEE/RSJ Int. Conf. Intell. Robot. Syst.*, vol. 3, no. October, pp. 2684–2689, 2002.

[4] S. Kuindersma, F. Permenter, and R. Tedrake, "An efficiently solvable quadratic program for stabilizing dynamic locomotion," *Proc. - IEEE Int. Conf. Robot. Autom.*, pp. 2589–2594, 2014.

[5] S. Kajita *et al.*, "Resolved momentum control: humanoid motion planning based on the linear and angular momentum," *Proc. 2003 IEEE/RSJ Int. Conf. Intell. Robot. Syst. (IROS 2003) (Cat. No.03CH37453)*, vol. 2, no. October, pp. 1644–1650, 2003.

[6] A. Goswami and V. Kallem, "Rate of change of angular momentum and balance maintenance of biped robots," *IEEE Int. Conf. Robot. Autom. 2004. Proceedings.*

[7] *ICRA '04. 2004*, no. April, p. 3785–3790 Vol.4, 2004.

[7] S. Feng, E. Whitman, X. Xinjilefu, and C. G. Atkeson, "Optimization-based full body control for the DARPA Robotics Challenge," *J. F. Robot.*, vol. 32, no. 2, pp. 293–312, 2015.

[8] X. Xinjilefu, V. Hayward, and H. Michalska, "Stabilization of the spatial double inverted pendulum using stochastic programming seen as a model of standing postural control," *9th IEEE-RAS Int. Conf. Humanoid Robot. HUMANOIDS09*, pp. 367–372, 2009.

[9] Z. Wang, M. Z. Chen, and J. Yi, "Soft robotics for engineers," *HKIE Transactions*, vol. 22, no. 2, pp. 88–97, 2015.

[10] Z. Wang, P. Polygerinos, J. T. Overvelde, K. C. Galloway, K. Bertoldi, and C. J. Walsh, "Interaction forces of soft fiber reinforced bending actuators," *IEEE/ASME Transactions on Mechatronics*, vol. 22, no. 2, pp. 717–727, 2017.

[11] J. Yi, X. Chen, C. Song, and Z. Wang, "Fiber-reinforced origami robotic actuator," *Soft robotics, 5(1), pp.81-92.* 2017, DOI: 10.1089. soro.2016.0079

[12] Y. Tian, K. Wang, J. Yi, Z. Wang, and M.Z. Chen, 2016, August. Introduction to modeling of the McKibben pneumatic artificial muscle with end constraints. In *Information and Automation (ICIA), 2016 IEEE International Conference on*(pp. 1624-1629). IEEE.

[13] X. Li, R. Wen, Z. Shen, Z. Wang, K. Luk, and Y. Hu, 2018, A Wearable Detector for Simultaneous Finger Joint Motion Measurement, *IEEE Transactions on Biomedical Circuits and Systems, in press, early available online*

[14] J. Yi, X. Chen, and Z. Wang, "A three-dimensional-printed soft robotic glove with enhanced ergonomics and force capability," *IEEE Robotics and Automation Letters*, vol. 3, no. 1, pp. 242–248, 2018.

[15] X. Chen, J. Peng, J. Zhou, Y. Chen, MY. Wang, and Z. Wang, 2017, May. A robotic manipulator design with novel soft actuators. In *Robotics and Automation (ICRA), 2017 IEEE International Conference on* (pp. 1878-1884). IEEE.

[16] J. Zhou, S. Chen, and Z. Wang, 2017. A Soft-Robotic Gripper With Enhanced Object Adaptation and Grasping Reliability. *IEEE Robotics and Automation Letters, 2*(4), pp.2287-2293.

[17] S. Kajita, F. Kanehiro, K. Kaneko, K. Yokoi, and H. Hirukawa, "The 3D linear inverted pendulum mode: a simple modeling for a biped walking pattern generation," *Proc. 2001 IEEE/RSJ Int. Conf. Intell. Robot. Syst. Expand. Soc. Role Robot. Next Millenn. (Cat. No.01CH37180)*, vol. 1, no. 4, pp. 239–246, 2001.

[18] S. Kajita and K. Tani, "Study of dynamic biped locomotion on rugged terrain-derivation and application of the linear inverted pendulum mode," *Proceedings. 1991 IEEE Int. Conf. Robot. Autom.*, no. April, pp. 1405–1411, 1991.

[19] S. H. Lee and A. Goswami, "Reaction Mass Pendulum (RMP): An explicit model for centroidal angular momentum of humanoid robots," *Proc. - IEEE Int. Conf. Robot. Autom.*, no. April, pp. 4667–4672, 2007.

[20] J. Pratt, J. Carff, S. Drakunov, and A. Goswami, "Capture point: A step toward humanoid push recovery," *Proc. 2006 6th IEEE-RAS Int. Conf. Humanoid Robot. HUMANOIDS*, vol. 207, no. 38, pp. 200–207, 2006.

[21] R. M. Murray and J. Hauser, "A case study in approximate linearization: The acrobot example," *Proc. Am. Control Conf.*, no. April, 1990.

[22] S. Collins, A. Ruina, R. Tedrake, and M. Wisse, "Efficient bipedal robots based on passive-dynamic walkers.," *Science*, vol. 307, no. 5712, pp. 1082–5, 2005.

[23] J. Park, "Synthesis of natural arm swing motion in human bipedal walking," *J. Biomech.*, vol. 41, no. 7, pp. 1417–1426, 2008.

[24] A. D. Kuo, "An Optimal Control Model for Analyzing Human Postural Balance," *IEEE Trans. Biomed. Eng.*, vol. 42, no. 1, pp. 87–101, 1995.

[25] M. W. Spong, "The Swingup Control Problem for the Acrobot," *IEEE Control Syst. Mag.*, vol. 15, no. May 1994, pp. 72–79, 1995.

[26] L. Wiklendt, S. Chalup, and R. Middleton, "A small spiking neural network with LQR control applied to the acrobot," *Neural Comput. Appl.*, vol. 18, no. 4, pp. 369–375, 2009.

[27] F. Xue, Z. Hou, and H. Deng, "Balance control for an acrobot," *Proc. 2011 Chinese Control Decis. Conf. CCDC 2011*, pp. 3426–3429, 2011.

[28] S. C. Brown and K. M. Passino, "Intelligent Control for an Acrobot," *J. Intell. Robot. Syst. Theory Appl.*, vol. 18, no. 3, pp. 209–248, 1997.

[29] D. C. Dracopoulos and B. D. Nichols, "Swing up and balance control of the acrobot solved by genetic programming," *Res. Dev. Intell. Syst. XXIX Inc. Appl. Innov. Intel. Sys. XX - AI 2012, 32nd SGAI Int. Conf. Innov. Tech. Appl. Artif. Intel.*, pp. 229–242, 2012.

[30] G. Boone, "Efficient Reinforcement Learning: Model-Based Acrobot Control," *Ieee Int. Conf. Robot. Autom.*, pp. 229–234, 1997.

[31] E. I. Butikov, "An improved criterion for Kapitza's pendulum stability," *J. Phys. A Math. Theor.*, vol. 44, no. 29, 2011.

[32] M. Bergerman, C. Lee, and Y. Xu, "Dynamic coupling of underactuated manipulators," *Control Appl. 1995., Proc. 4th IEEE Conf.*, pp. 500–505, 1995.

[33] J. Pratt, C. M. Chew, A. Torres, P. Dilworth, and G. Pratt, "Virtual model control: an intuitive approach for bipedal locomotion," *Int. J. Rob. Res.*, vol. 20, no. 2, pp. 129–143, 2001.

[34] E. I. Butikov, "On the dynamic stabilization of an inverted pendulum," *Am. J. Phys.*, vol. 69, no. 7, pp. 755–768, 2001.

[35] B. Ahmad and S. Borisenok, "Control of effective potential minima for Kapitza oscillator by periodical kicking pulses," *Phys. Lett. Sect. A Gen. At. Solid State Phys.*, vol. 373, no. 7, pp. 701–707, 2009.

[36] R. M. Murray and S. S. Sastry, "Nonholonomic motion planning. Steering using sinusoids," *IEEE Trans. Automat. Contr.*, vol. 38, no. 5, pp. 700–716, 1993.